

# Loki: a ground-layer adaptive optics high-resolution near-infrared survey camera

Christoph Baranec, Michael Lloyd-Hart, and Michael Meyer  
Center for Astronomical Adaptive Optics, Steward Observatory,  
933 N. Cherry Ave., Tucson, AZ, 85721

## ABSTRACT

We present the design of a new high-resolution near-infrared survey camera that will take advantage of the wide corrected field afforded by the 6.5 m MMT's new multi-laser ground-layer adaptive optics (GLAO) system. GLAO technology will correct for turbulence close to the telescope aperture where typically 1/2 to 2/3 of the total atmospheric turbulence lies and is expected to deliver image widths of 0.1-0.2 arc seconds in the near-infrared across a wide range of seeing conditions. The new camera will use a 2 by 2 mosaic of JWST NIRCcam detectors, 2048 x 2048 arrays sensitive from 0.6 - 2.5  $\mu\text{m}$  based on Teledyne's HgCdTe HAWAII-2RG detector technology. The camera has a 4 arc minute square field, giving a plate scale of approximately 0.06 arc seconds/pixel, critically sampling the GLAO PSF. In addition, high resolution (0.25 arc seconds or better) multi-object spectroscopy can be supported with cold slit masks inside the dewar; allowing potentially hundreds of spectra to be obtained at once with resolutions of up to 10,000.

**Keywords:** adaptive optics, infrared instrumentation, multi-object spectroscopy

## 1. INTRODUCTION

With the MMT laser guide star (LGS) AO system now on the verge of giving partial correction over a wide field in ground-layer adaptive optics (GLAO) mode<sup>1</sup>, one of the next priorities is to use this powerful new technique to support science. From open-loop wavefront measurements with the instrument<sup>2,3</sup>, ground-layer adaptive optics correction is expected to routinely have  $< 0.2$  arc second FWHM PSFs in K band ( $\lambda = 2.2 \mu\text{m}$ ) over a 2+ arc minute field. With future improvements to software and hardware, imaging performance should further improve. Potentially, all of the current MMT AO instruments can benefit from using the laser guide star AO system, provided the installation of larger entrance window dichroics, as has been done with PISCES<sup>4</sup> and Clio<sup>5,6</sup>. The laser AO system alleviates the need to have a bright,  $m_v < 13$ , science target or nearby guide star. In these cases the laser AO system could be run in one of two modes, the proven ground-layer AO mode, giving partial correction over a wide field, or the tomographic AO (LTAO) mode, which will be demonstrated in 2008, but capable of giving diffraction limited imaging along a particular line of sight. Obviously, the narrow field MMT AO instruments, Clio, ARIES<sup>7</sup> and BLINC-MIRAC<sup>8</sup>, would be much better suited to tomographic AO correction; however in the thermal bands, ground-layer AO can give significant Strehl improvement which may be useful until tomographic correction is fully realized.

Currently PISCES is the only instrument well matched to the ground-layer AO corrected field. It has a 110 square arc second field with a plate scale of 0.11 arc seconds per pixel. From previous open-loop experiments<sup>2</sup> it has been found that the GLAO corrected field can extend beyond the beacon diameter in cases where the ground-layer is low, with faster roll-off of correction as the mean height of the ground layer increases. This means that even with the current configuration of the MMT LGS constellation diameter of 2 arc minutes, there is potentially a larger GLAO corrected field that could be of use to science instruments. In addition, there are future plans to upgrade the MMT LGS AO instrument to accommodate an additional three laser heads and have a beacon diameter which can be adjusted up to 5 arc minutes, ideal for GLAO, and to a narrow field ideal for LTAO. In this future AO wavefront sensing instrument the GLAO corrected field would be potentially 5 arc minutes in diameter, much larger than any current MMT AO instrument can explore. This leads naturally to the idea of building a camera which can take advantage of such a large AO corrected field. Having this capability would give the MMT a competitive edge over many other larger telescopes in the world.

For ground based background limited surveys in the near-infrared, the signal-to-noise ratio (SNR) for a stellar source is proportional to the diameter of the telescope divided by the image width. The total time necessary to complete the same size and SNR survey is inversely proportional to the SNR times the solid angle. With the given PSF diameter of the GLAO corrected images at the MMT, and the field of the new instrument, the GLAO camera is expected to have a higher scientific throughput than any of the seeing limited instruments at the largest telescopes in the world. Table 1 shows the relative time needed for surveys at current telescopes and what is expected with a new imaging camera using the MMT laser AO system.

Table 1. Comparisons of the total telescope time needed for the same surveys. \*Image widths are calculated assuming excellent seeing of  $r_0=22.5$  cm at 500 nm, and GLAO performance presented in the following section. In worse seeing, seeing limited image widths will increase while GLAO images will remain similar in size, so these are conservative estimates.

Telescope	Instrument	D (m)	K-FWHM* (arcsec)	Relative SNR	$\Omega$ (arcmin <sup>2</sup> )	Relative Exp. Time
Gemini	NIRI	8.01	0.34	1	4	8
VLT	ISAAC	8	0.34	1	6.4	5
Subaru	MOIRCS	8.2	0.34	1	28	1.14
MMT	Loki / GLAO	6.3	0.13	2	16	1

## 2. MMT MULTIPLE LASER AO SYSTEM

The 6.5 m MMT is so far the only telescope in the world to implement multi-laser adaptive optics wavefront sensing<sup>2, 9</sup>. One of the many AO correction modes this system supports is ground layer adaptive optics (GLAO), first suggested by Rigaut<sup>10</sup> in 2002. By averaging the wavefronts of multiple laser guide stars over a wide field of view, one can calculate an estimate of the errors introduced by the ground layer. Compensating for this error with a deformable mirror conjugated close to the telescope's entrance pupil will partially correct the wavefronts from all objects in the field of view simultaneously. It has been found empirically at the MMT and other sites that the contribution to wavefront error of the ground is typically from 1/2 to 2/3 of overall turbulence<sup>2, 9, 11-18</sup>, so GLAO will be particularly powerful at improving imaging over wide fields.

The laser AO system at the MMT comprises five beacons, generated by Rayleigh scattering, with two commercial, pulsed doubled-YAG lasers at 532 nm. The five beacons, each with a projected power of 4 W, are arranged in a regular pentagon of 2 arc minutes diameter. The images from all five beacons are recorded on a novel implementation of the Shack-Hartmann wavefront sensor (WFS), which includes the dynamic focus optics and a single electronically shuttered CCD. A prism array at the exit pupil divides it into 60 subapertures of equal area arranged in a hexapolar geometry. In addition, there is a camera which measures the image motion of a single star in the science field to correct for tilt errors over the entire field.

Over the past two years, open-loop measurements using the laser AO system have been performed, allowing characterization of atmospheric parameters specific to the MMT and evaluation of different modes of the AO system when used in closed-loop with the deformable secondary. The following results are reproduced in summary from Lloyd-Hart et al.<sup>19</sup> In an experiment at the MMT in June 2005, data was collected that let us predict the closed-loop GLAO performance we expect to achieve. GLAO wavefront corrections of Zernike orders 2 through 6 were calculated from the LGS, assuming a temporal lag of 0.02 s. To the corrected stellar wavefronts were added random amounts of Zernike orders 7 through 100 drawn from an uncorrected Kolmogorov distribution. Synthetic residual tilt errors were also added assuming that global image motion was measured from a stellar source at the center of the field, with noise and anisoplanatic errors determined empirically from separate observations of a five-star asterism with a separate wide field camera. Figure 1 shows an example of the uncorrected and GLAO corrected K band PSFs for a star near the center of the LGS constellation. Table 2 summarizes a number of measures of image quality calculated from these synthetic PSFs in K and H ( $\lambda = 1.65 \mu\text{m}$ ) band.

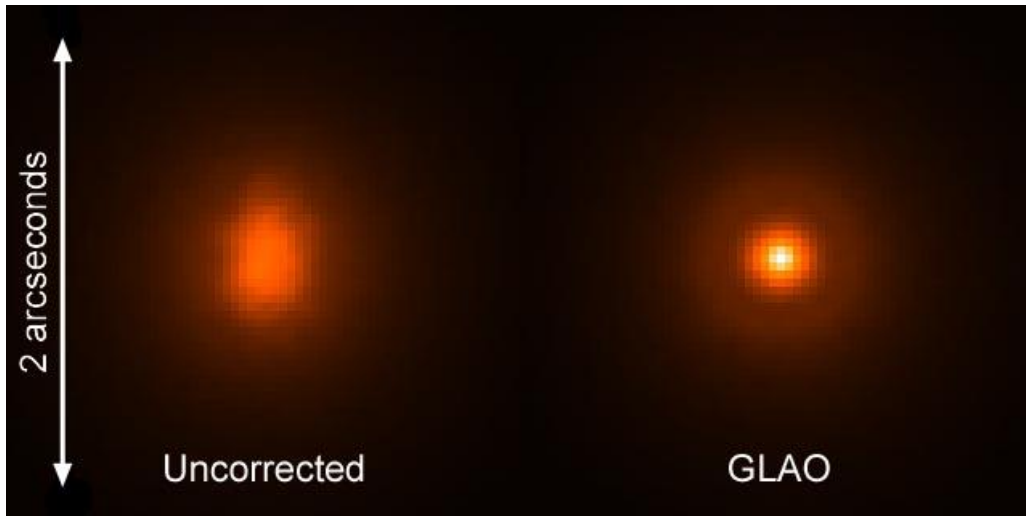


Fig. 1. Synthetic point-spread functions computed at 2.2  $\mu\text{m}$  wavelength from wavefronts before and after GLAO correction for a star in the center of the LGS constellation over a 60 s period.

Table 2. Radially averaged quality metrics computed for synthetic GLAO PSFs from open-loop wavefront data. Results are shown for field angles of 5, 25, and 50 arcsec in both H and K bands.

Metric	Field angle (arc sec)						Diffraction Limit		Seeing limit ( $r_0 = 22.5$ cm)	
	5		25		50		H	K	H	K
FWHM (arcsec)	0.10	0.10	0.13	0.12	0.14	0.13	0.052	0.070	0.36	0.34
$\theta_{50}$ (arcsec)	0.21	0.13	0.21	0.14	0.21	0.14	0.048	0.064	0.27	0.25
$\theta_{80}$ (arcsec)	0.51	0.46	0.51	0.47	0.51	0.47	0.095	0.13	0.52	0.51
Peak Intensity	0.082	0.21	0.056	0.16	0.055	0.14	1.0	1.0	0.015	0.028

Analysis of the average power in the Zernike modes of the NGS wavefronts shows that the mean  $r_0$  was 22.5 cm at 500 nm with an outer scale  $L_0$  of 19 m. Even though the seeing was already excellent, GLAO further improved the resolution, to within about a factor 2 of the diffraction limit. The 50% encircled energy radius  $\theta_{50}$  also saw substantial improvement, particularly in the K band. Furthermore, the variability of the PSF over the explored field, with a radius of 50 arc seconds, is remarkably small.

While these results by themselves are encouraging, we find that the value of GLAO is not restricted to periods when the seeing is already good. Unlike conventional AO where the diffraction limit is the goal, the more modest reach of GLAO is also more robust to adverse atmospheric conditions. Data from a period when the value of  $r_0$  was 10.1 cm, approximately half the value for the results above and at the site's 75<sup>th</sup> percentile, show that improvement of the K-band PSF to FWHM of 0.2 arc seconds will still be possible under such conditions.

For the first time, we expect to close the full high order GLAO control loop around the five laser beacons and a tilt star at the MMT in October 2007<sup>1</sup>. We intend to explore the image quality, stability and sensitivity of GLAO correction as a function of waveband with PISCES which is well matched to the expected FWHM performance of the GLAO corrected field and will be able to examine PSF non-uniformity and temporal stability across a wide field.

### 3. SCIENTIFIC APPLICATIONS

There are countless numbers of science programs where the ability to do deep wide-field imaging and spectroscopy is important. As an example, near infrared observations of high redshift galaxies could be particularly interesting as current

ground based optical observations and thermal infrared data from Spitzer leave a gap at 1-3  $\mu\text{m}$ . Adding near infrared to the spectral energy distributions is important for photometric redshifts and stellar population inferences, while near infrared imaging is important to assess the morphology of the older stars. With present technology, the optical and Spitzer data are far faster to acquire, i.e., the near infrared imaging is the bottleneck for acquiring pan-chromatic data on high redshift galaxies. The new instrument Loki paired with the MMT GLAO system offers the chance of having consistently good imaging quality, well matched to the sizes of high redshift galaxies, to integrate down to the required faint flux levels. This is particularly true in K band, where GLAO will perform well and where Hubble Space Telescope has little capability.

With the integration of multi-object spectrographic (MOS) capability, the spectra of hundreds of these same high redshift galaxies could be captured over the 16 square arc minute field with resolutions of up to 10,000. With 0.25 arc second or smaller slits, and 0.1 to 0.2 arc second resolution, well matched to the GLAO PSF, the extended source galaxies will be well resolved both spatially and spectrally.

With the increased sensitivity and resolution afforded to this instrument with the GLAO system, large portions of the sky can be quickly imaged. In just a few nights NGC 1333 could be covered down to the required sensitivity in J ( $\lambda = 1.25 \mu\text{m}$ ), H and K bands of  $2 M_{\text{Jupiter}}$  at  $10 \sigma$ , covering the high column density cloud material as well as all stars that could have drifted off the cloud within 1-2 Myr of their formation (assuming 1 km/s peculiar motion). With on-sky spatial resolution of  $\sim 0.13$  arc seconds, objects can be resolved as little as 40 AU apart in NGC 1333 (300 pc), close to the peak of the binary separation distribution.

With a deep survey of NGC 1333, the stellar and sub-stellar objects within the cloud can be categorized and the spatial effects on their distribution investigated. For each object, the presence of a circumstellar dust disk can be detected, which is a precursor for associated planetary bodies. This can be done by looking in the K band where the disk causes an excess in luminosity. Because the dust is transparent for wavelengths shorter than K, a color-magnitude diagram for each source can be made using observations in J and H. On the color-magnitude diagram, an extinction limited sample can be created by over-plotting the isochrone for a zero age main sequence star and using a reddening vector out to the sensitivity limit. The numbers of objects over given mass ranges can then be counted, and the ratios of stars to low-mass objects, and low-mass stars to brown dwarfs can be calculated. With the wide field of view, it can be seen if these ratios change significantly as different parts of the cluster are probed. These results will be compared to studies of other clusters.

For any given sample set of objects, the number of objects can be counted within a certain mass range and an initial mass function (IMF) calculated. The IMF for different parts of the cluster will be calculated by selecting stellar regions of different radii. Using a cumulative distribution function on the masses and number of objects, the Kolmogorov-Smirnov test<sup>20</sup> can be used to see if there are characteristic anisotropies in the IMF.

From these populations of different objects, it can be seen if there is any mass segregation between high and low mass objects. Mass segregation in older clusters is expected to be seen, either through collisions<sup>21</sup> or high mass objects collecting in the center and ejecting lower mass objects. However, as in some young clusters like the Trapezium, there are strong signs of mass segregation. Observations with Loki will be able to determine if there is mass segregation also occurring within the young cluster NGC 1333, and possibly what may be the cause.

In a long term observing plan, the survey should be repeated approximately 5 years after the initial survey. Proper motions of objects in excess of 50 km/s would then be detected. In conjunction with follow-up spectroscopy measurements, a velocity distribution map of fast moving members of the cluster could be made. With N-body simulations, the evolution of the distribution of objects could be then tracked.

It is expected that there will be regions of excess of low-mass objects based on the results by Greissl et al. 2007<sup>22</sup>. This will confirm the previous observations, and possibly change the understanding of how low-mass objects form in clusters. Any IMF anisotropies will be detected across the cluster which may be affecting the mass ratios observed.

#### 4. CAMERA DESIGN

There are a number of requirements for the optical design of Loki, the science camera that will work behind the MMT's ground-layer AO system. The main advantage of GLAO is the consistent AO correction over a wide field, and the camera should image a large portion of that field. The expected FWHM of the corrected images will be around 0.1 – 0.2 arc seconds in diameter, and the plate scale of the camera should be smaller than this, optimally nyquist sampled at 0.05 arc seconds per pixel. Access to the focal plane is necessary for the slit masks and any calibration sources. There should be a location in the camera to place filters and a grism for MOS mode; ideally this spot should be as small as possible since larger filters are more expensive. This location would also be an ideal place to put a cold stop if observations at wavelengths greater than  $K_{\text{short}}$  ( $\lambda \sim 2.1 \mu\text{m}$ ) are desired. The optical design should also be achromatic over the range of wavelengths in the near infrared (1 – 2.5  $\mu\text{m}$ ).

The design of Loki was first constrained by the available detectors. Steward Observatory has access to a number of the detectors used in the JWST NIRCam instrument project<sup>23</sup>, which are based on Rockwell Scientific's HgCdTe HAWAII-2RG detector technology, and are  $2048 \times 2048$  arrays sensitive from 0.6 – 2.5  $\mu\text{m}$ . By using a 2 by 2 mosaic of these devices there will be a total of  $4096 \times 4096$  pixels. Taking a 4 arc minute square field imaged onto the detector gives a plate scale of approximately 0.06 arc seconds per pixel, critically sampling the GLAO PSF. This gives both a large field and high resolution plate scale.

The rest of the optical design was based on converting the incoming F/15 light to an F/ratio of 9.8 and accommodating the other design requirements. The initial design was based on a modified offner relay that had a non 1:1 magnification ratio. Using an offner design allows for the use of mirrors, immediately solving the achromatic requirement. The design was modeled in Zemax and optimum design found. A conceptual optical design of Loki appears in figure 2. Note that all of the optics are spherical, eliminating the extra manufacturing time and cost associated with aspheric optics.

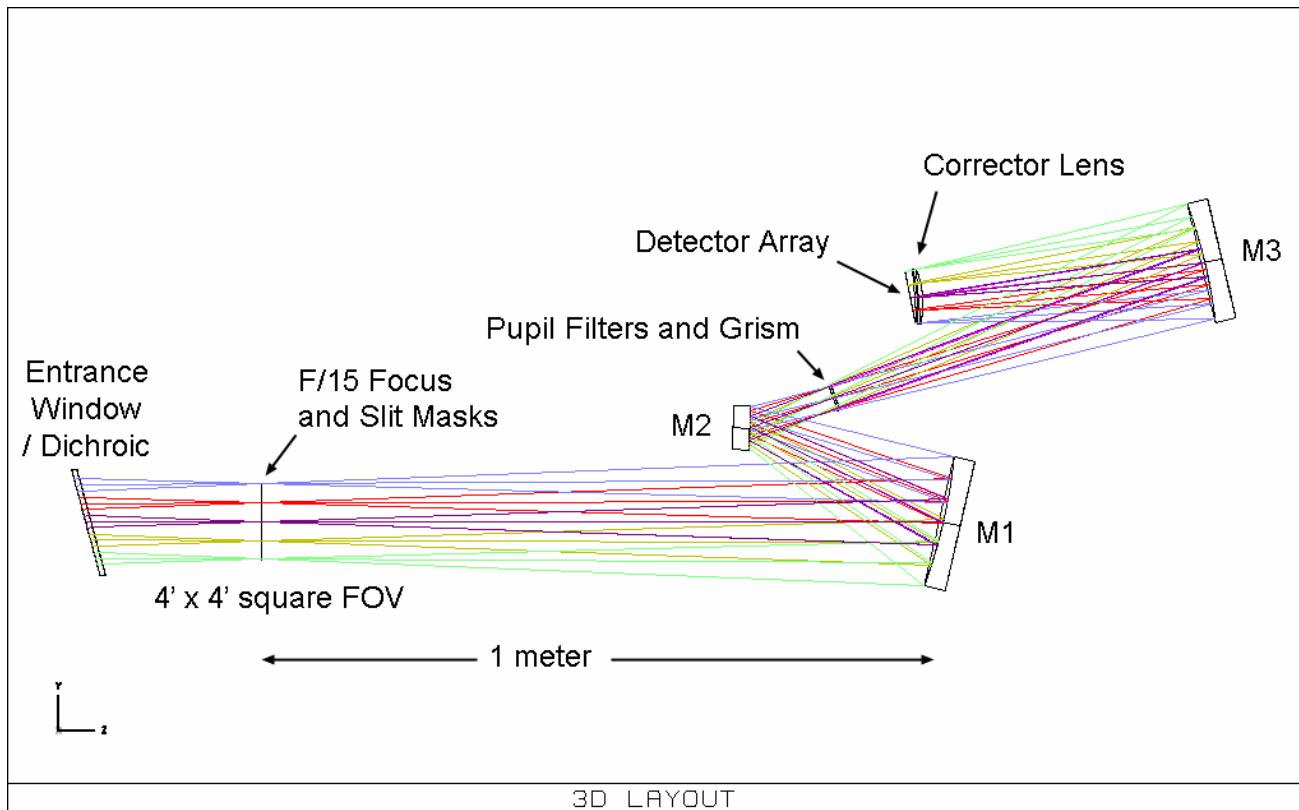


Fig. 2. Non-folded optical layout of Loki. The F/15 secondary would be to the left on this figure.

The first element is the entrance window made of CaF<sub>2</sub>. This also doubles as a dichroic, much like the ones on the current MMT AO science instruments, to split off the visible light to the wavefront sensors in the laser AO system. Internally there is an image plane 250 mm behind the entrance window. This is an ideal place to insert cold slit masks for the MOS mode of Loki. A cold robotic cassette, similar to the one used in the Large Binocular Telescope's LUCIFER instrument<sup>24</sup> could be utilized. In addition, fiber sources can be placed here for both spectral and distortion calibration. The first mirror, M1, is located 1 m behind the focus. In actual operation, the optical design will be folded up to reduce the amount of volume occupied, as opposed to what is seen in figure 2. M1 and M2 together form a pupil where filters and a grism for the MOS mode can be placed. Figure 3 shows the footprint of the pupil as seen from the full field points at this location. The pupil is contained within a 44 mm diameter extent, so standard 50 mm filters can be used. M3 reimages the light from the pupil to the detector plane which is tilted. A corrector lens, also made of CaF<sub>2</sub>, is placed in front of the detector to minimize field curvature. The image quality at J band is seen in figure 4 for the center, edge and corners of the 4 arc minute field. The image is essentially diffraction limited except at the very corners of the field. With ~ 20 μm pixels, this imaging quality is more than sufficient. The prescription for the system is seen in table 3. There is still some residual distortion that can be seen in the optical design. This can be seen in figure 5. The maximum amount of distortion is 4.4 % at two corners of the field.

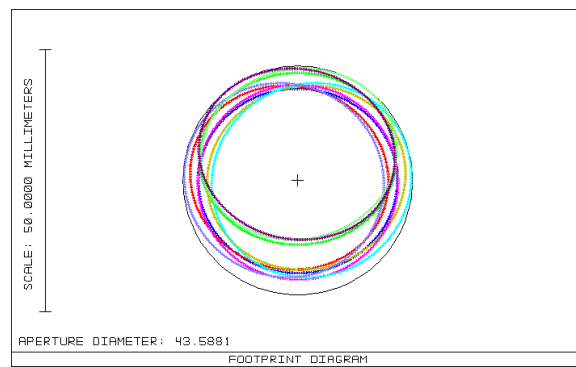


Fig. 3. Footprint diagram showing the pupil from the central and edge field points. Each colored ring represents the extent of light from each field point.

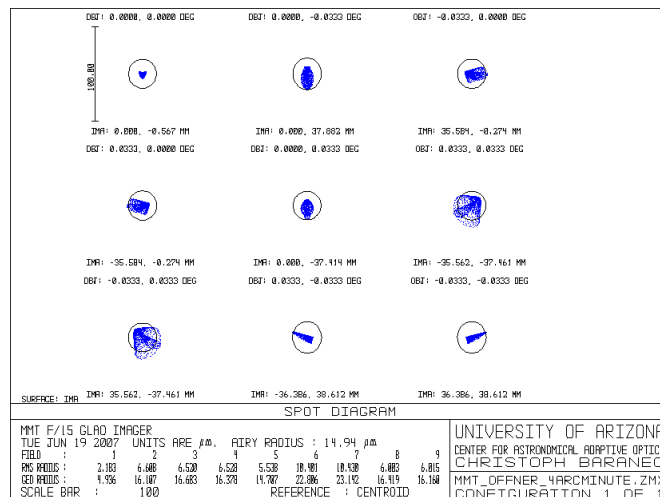


Fig. 4. J band spot diagrams for on-axis, edge (2 arc minutes) and corner (2.8 arc minutes) field points. The black circle represents the FWHM of the airy disk core. For the longer wavelengths, the spot diagrams remain the same while the airy disk increases in size.

Table 3. Optical prescription for the GLAO instrument Loki.

#	Surface type	Comment	R.O.C. (mm)	Thickness (mm)	Glass	Aperture radius (mm)	Conic
0	Std.			Infinity			
1	Std.	Secondary shadow		7200.00		3217.3	
2	Std.	Primary mirror	-16256	-7307.47	Mirror	3251.0	-1.000
3	Std.	Secondary mirror	-1794.5486	7307.47	Mirror	321.0	-1.409
4	Std.	Primary vertex		1467.07		118.4	
5	Std.	Derotator		381.00		850.0	
6	Std.	WFS inst. floor		180.09		67.4	
7	Std.	Instrument dichroic		8.00	CaF <sub>2</sub>	65.1	
8	Std.	F/15 focus		1250.76		65.6	
9	Coordbrk.	(Tilt 13°)					
10	Std.	M1	-779.1753		Mirror	96.8	
11	Coordbrk.	(Tilt 13°)		-315.19			
12	Coordbrk.	(Tilt -23°)					
13	Std.	M2	-575.3564		Mirror	32.2	
14	Coordbrk.	(Tilt -23°)		129.44			
15	Std.	Pupil filters		3.50	CaF <sub>2</sub>	20.1	
16	Std.			577.29		20.3	
17	Coordbrk.	(Tilt 6.61°)					
18	Std.	M3	-767.0732		Mirror	89.3	
19	Coordbrk.	(Tilt 6.61°)		-417.48			
20	Coordbrk.	(Tilt 2.17°)					
21	Std.	Corrector lens	-137.0158	-8.00	CaF <sub>2</sub>	40.8	
22	Std.		-230.5528			39.7	
23	Coordbrk.	(Tilt -2.17°)		-10.00			
24	Coordbrk.	(Tilt -4.60°)					
25	Std.	Detector array				38.1	

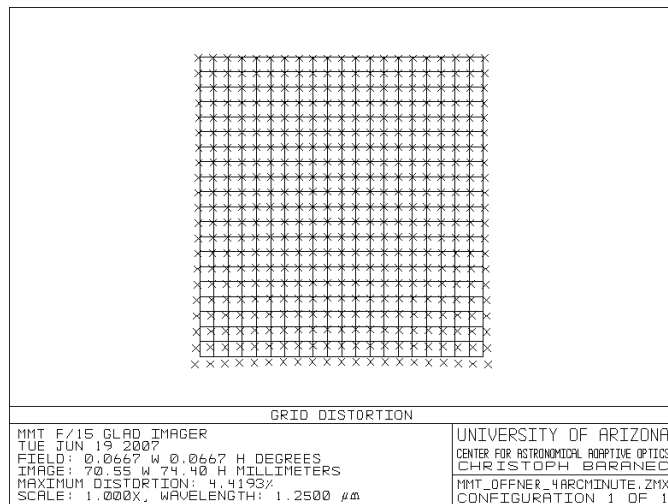


Fig. 5. Grid distortion diagram of the 4 arc minute square field on the detector.

Since the instrument will be working in the near infrared, it will need to be housed in an evacuated and cooled dewar. As mentioned, the dichroic will also act as the entrance window to a dual-vessel system where the external chamber is a simple liquid nitrogen vessel that cools a cold plate upon which all of the optics are mounted. The interior vessel will be isolated from the rest of the instrument and control only the detector's temperature. The option will be available to pump on the nitrogen to achieve temperatures below 77K which may be used to help reduce the dark current of the detectors. A vapor cooled shield will be located around both vessels to increase the hold times.

## 5. CONCLUSIONS AND FUTURE WORK

With an initial working design finished and a near operational ground-layer AO system at the MMT, there should be nothing stopping the on-going development of Loki. The MMT, with a new wide field camera that exploits this technology, is poised to become the first telescope to take full advantage of ground-layer AO correction and enable a new round of deep wide-field science that will not be available at other telescopes for numerous years.

There are still refinements that need to be addressed in the system. Although the imaging characteristics of the optical design perform to specifications, flattening of the pupil is necessary if imaging is desired into the thermal K band and beyond; however the selected detectors are only sensitive out to 2.5  $\mu\text{m}$ . Once flat, a cold stop can be located at the pupil along with the filters. Details of the calibration of both the optical distortion and spectral response of the MOS mode still need to be investigated. The optical design has yet to be folded to decrease its volume and will then need to be appropriately baffled. Another feature that would be advantageous to the instrument would be the ability to change to a diffraction limited plate scale. If there was any desire to take higher resolution images of specific targets on the fly, this could be done by switching the MMT laser AO system over to LTAO mode, by simply changing the reconstructor matrix used in the real-time control computer.

We are grateful for assistance from Phil Hinz regarding the optical design. This work has been supported by the National Science Foundation under grant AST-0505369.

## REFERENCES

1. C. Baranec, M. Lloyd-Hart, N. M. Milton, T. Stalcup, M. Snyder, V. Vaitheeswaran, D. McCarthy & R. Angel, "Astronomical imaging using ground-layer adaptive optics," these proceedings.
2. M. Lloyd-Hart, C. Baranec, N. M. Milton, M. Snyder, T. Stalcup & R. Angel, "Experimental results of ground-layer and tomographic wavefront reconstruction from multiple laser guide stars," *Opt. Express* 14, 7541-7551 (2006).
3. C. Baranec, M. Lloyd-Hart, N. M. Milton, T. Stalcup, M. Snyder & R. Angel, "Tomographic reconstruction of stellar wavefronts from multiple laser guide stars," *Proc. SPIE Advances in Adaptive Optics II*, eds. B. Ellerbroek & D. B. Calia, 6272 (2006).
4. D. McCarthy, J. Ge, J. Hinz, R. Finn & S. de Jong, "PISCES: A Wide-Field, 1-2.5  $\mu\text{m}$  Camera for Large-Aperture Telescopes," *Publ. Astron. Soc. Pac.* 113, 353-361 (2001).
5. M. Freed, P. Hinz, M. Meyer, N. M. Milton & M. Lloyd-Hart, "Clio: A 5 micron camera for the detection of giant exoplanets," *Proc. SPIE Ground-based Instrumentation for Astronomy*, eds. A. Moorwood & M. Iye, 5492, 1561-1571 (2004).
6. S. Sivanandam, P. Hinz, A. Heinze, M. Freed & A. Breuninger, "Clio: a 3-5 micron AO planet-finding camera," *Proc. SPIE Ground-based and Airborne Instrumentation for Astronomy*, eds. I. McLean & M. Iye, 6269 (2006).
7. D. McCarthy, J. Burge, R. Angel, J. Ge, R. Sarlot, B. Fitz-Patrick & J. Hinz, "ARIES: Arizona infrared imager and echelle spectrograph," *Proc. SPIE Infrared Astronomical Instrumentation*, ed. A. Fowler, 3354, 750-754 (1998).
8. P. Hinz, R. Angel, N. Woolf, W. Hoffmann & D. McCarthy, "BLINC: a testbed for nulling interferometry in the thermal infrared," *Proc. SPIE Interferometry in Optical Astronomy*, eds. P. Lena & A. Quirrenbach, 4006, 349-353 (2000).
9. M. Lloyd-Hart, C. Baranec, N. M. Milton, T. Stalcup, M. Snyder, N. Putnam, & J. R. P. Angel, "First tests of wavefront sensing with a constellation of laser guide beacons," *Astrophys. J.* 634, 679-686 (2005).
10. F. Rigaut, "Ground-conjugate wide field adaptive optics for the ELTs," *Proc. ESO Beyond Conventional Adaptive Optics*, eds. E. Vernet, R. Ragazzoni, S. Esposito & N. Hubin, 58, 11-16 (2002).

11. C. Baranec, M. Lloyd-Hart & N. M. Milton, "Ground-layer wave front reconstruction from multiple natural guide stars," *Astrophys. J.* 661, 1332-1338 (2007).
12. D. Andersen, J. Stoesz, S. Morris, M. Lloyd-Hart, D. Crampton, T. Butterley, B. Ellerbroek, L. Jollissaint, N. M. Milton, R. Myers, K. Szeto, A. Tokovinin, J.-P. Veran & R. Wilson, "Performance Modeling of a Wide-Field Ground-Layer Adaptive Optics System," *Publ. Astron. Soc. Pac.* 118, 1574-1590 (2006).
13. R. Avila, E. Masciadri, J. Vernin & J. Sánchez, "Generalized SCIDAR Measurements at San Pedro Mártir. I. Turbulence Profile Statistics," *Publ. Astron. Soc. Pac.* 116, 682-692 (2004).
14. S. Egner, E. Masciadri, D. McKenna, T. M. Herbst & W. Gaessler, "G-SCIDAR measurements on Mt. Graham - recent results," *Proc. SPIE Advances in Adaptive Optics II*, eds. B. Ellerbroek & D. B. Calia, 6272 (2006).
15. A. Tokovinin & T. Travouillon, "Model of optical turbulence profile at Cerro Pachón," *Mon. Not. R. Astron. Soc.*, 365, 1235-1242 (2006).
16. A. Tokovinin, J. Vernin, A. Ziad & M. Chun, "Optical Turbulence Profiles at Mauna Kea measured by MASS and SCIDAR," *Publ. Astron. Soc. Pac.* 117, 395-400 (2005).
17. V. Velur, R. Flicker, B. Platt, M. Britton, R. Dekany, M. Troy, J. Roberts, J. Shelton & J. Hickey, "Multiple guide star tomography demonstration at Palomar Observatory," *Proc. SPIE Advances in Adaptive Optics II*, eds. B. Ellerbroek & D. B. Calia, 6272 (2006).
18. J. Verin, A. Agabi, R. Avila, M. Azouit, R. Conan, F. Martin, E. Masciadri, L. Sanchez, & A. Ziad, "Gemini site testing campaign. Cerro Pachon and Cerro Tololo," Gemini RPT-AO-G0094, <http://www.gemini.edu/> (2000).
19. M. Lloyd-Hart, T. Stalcup, C. Baranec, N. M. Milton, M. Rademacher, M. Snyder, M. Meyer & D. Eisenstein, "Scientific goals for the MMT's multi-laser-guided adaptive optics," *Proc. SPIE Advances in Adaptive Optics II*, eds. B. Ellerbroek & D. B. Calia, 6272 (2006).
20. I. Chakravarti, R. Laha, & J. Roy, *Handbook of Methods of Applied Statistics. Vol. I: Techniques of Computation, Descriptive Methods and Statistical Inference*, (Wiley, 1967), 392-394.
21. I. Bonnell & M. Bate, "Accretion in stellar clusters and the collisional formation of massive stars," *Mon. Not. R. Astron. Soc.* 336, 659 (2002).
22. J. Greissl, M. Meyer, B. Wilking, T. Fanetti, G. Schneider, T. Greene & E. Young, "HST/NICMOS Observations of NGC 1333: The Ratio of Stars to Sub-stellar Objects," *Astron. J.* 133, 1321-1330 (2007).
23. E. Young, M. Rieke, D. Hall, J. Garnett, M. Loose, A. Magoncelli & G. Winters, "Detectors for the NIRCAM Instrument on JWST," *Bulletin AAS* 207, 115 (2006).
24. H. G. Mandel, I. Appenzeller, W. Seifert, H. Baumeister, R.-J. Dettmar, C. Feiz, H. Gemperlein, A. Germeroth, B. Grimm, J. Heidt, T. Herbst, R. Hofmann, M. Jütte, V. Knierim, W. Laun, T. Luks, M. Lehmitz, R. Lenzen, K. Polsterer, A. Quirrenbach, R.-R. Rohloff, J. Rosenberger, P. Weiser, & H. Weisz, "LUCIFER status report: Summer 2006," *Proc. SPIE Ground-based and Airborne Instrumentation for Astronomy*, eds. I. S. McLean & M. Iye, 6269 (2006).